

Elsevier Editorial System(tm) for Composites Part B  
Manuscript Draft

Manuscript Number:

Title: Multi-functional Hindered Amine Light Stabilizers functionalized Carbon Nanotubes for advanced Ultra-High Molecular Weight Polyethylene-based Nanocomposites

Article Type: Full Length Article

Keywords: A. Polymer-matrix composites (PMCs)

A. Nano-structures

B. Physical properties

B. Rheological properties

B. Mechanical properties

Corresponding Author: Prof. Nadka Tzankova Dintcheva,

Corresponding Author's Institution: Università di Palermo

First Author: Nadka Tzankova Dintcheva

Order of Authors: Nadka Tzankova Dintcheva; Rossella Arrigo; Elisabetta Morici; Cristian Gambarotti; Sabrina Carroccio; Francesca Cicogna; Giovanni Filippone

Abstract: Hindered Amine Light Stabilizer (HAS) molecules were covalently linked onto outer surface of multi-walled carbon nanotubes (CNTs) and the obtained multi-functional fillers (HAS-f-CNTs) were dispersed in Ultra High Molecular Weight Polyethylene (UHMWPE) aiming at obtaining advanced nanocomposites with enhanced photo-oxidative stability, electrical and mechanical properties. The effective grafting of HAS molecules is confirmed by spectroscopic, spectrometric and thermo-gravimetric analyses, and the influence of the multi-functional nanoparticles on the morphology, mechanical and electric behaviour and photo-oxidative stability of the nanocomposites are investigated. UHMWPE/HAS-f-CNTs nanocomposite shows improved electrical and mechanical properties compared with those of bare CNTs based nanocomposites and, due to the multi-functional nature of used nanoparticles, shows enhanced photo-oxidative stability caused by a synergic action between the immobilized HAS molecules and the radical scavenging activity of CNTs.

Suggested Reviewers: Pieter Gijsman  
pieter.gijsman@dsm.com

Vincenzo Malatesta  
malatesta\_vincenzo@fastwebnet.it

Opposed Reviewers:



UNIVERSITÀ  
DEGLI STUDI  
DI PALERMO

DIPARTIMENTO DI INGEGNERIA CIVILE,  
AMBIENTALE, AEROSPAZIALE, DEI MATERIALI



Palermo, 30/01/2015

**To: Prof. L. Feo,  
Editor for Europe**

**From: Prof. N.Tz. Dintcheva  
University of Palermo**

Dear Editor,

Enclosed please find the manuscript entitled “Multi-functional Hindered Amine Light Stabilizers-functionalized Carbon Nanotubes for advanced Ultra-High Molecular Weight Polyethylene-based Nanocomposites”, to be considered for publication in Composites part B - Engineering.

We report about advanced Ultra-High Molecular Weight Polyethylene (UHMWPE)-based Nanocomposites with enhanced photo-oxidative stability, electrical and mechanical properties achieved through multi-functional fillers adding. In particular, Hindered Amine Light Stabilizer (HAS) molecules were covalently linked onto outer surface of multi-walled carbon nanotubes (CNTs) and the obtained multi-functional fillers (HAS-*f*-CNTs) were dispersed in the host polymeric matrix. To confirm the effective grafting of HAS molecules onto CNTs spectroscopic, spectrometric and thermo-gravimetric analyses has been accurately performed and discussed. Besides, the influence of the multi-functional nanoparticles on the morphology, mechanical and electric behaviour and photo-oxidative stability of the nanocomposites were investigated. UHMWPE/HAS-*f*-CNTs nanocomposite shows improved electrical and mechanical properties compared with those of bare CNTs based nanocomposites and, due to the multi-functional nature of used nanoparticles, shows enhanced photo-oxidative stability caused by a synergic action between the immobilized HAS molecules and the radical scavenging activity of CNTs.

Concluding, we believe that our results can be potentially extended to many other systems; the CNTs can be profitably used as a substrate on which grafting molecules carrying specific functionality. Furthermore, it is important to note that the approach is quite general, and the nature of both functional molecules and nanoparticles can be properly selected to design polymer materials for demanding applications.

We hence believe that our manuscript may be suitable for publication in Composites part B - Engineering, and we shall welcome any comments you or your Referees may have about our work.

Sincerely yours,

Prof. N.Tz. Dintcheva

1 **Multi-functional Hindered Amine Light Stabilizers-functionalized**  
2  
3  
4 **Carbon Nanotubes for advanced Ultra-High Molecular Weight**  
5  
6  
7 **Polyethylene-based Nanocomposites**  
8  
9

10  
11  
12  
13  
14 **N. Tz. Dintcheva<sup>\*1</sup>, R. Arrigo<sup>1</sup>, E. Morici<sup>1</sup>, C. Gambarotti<sup>2</sup>, S. Carroccio<sup>3</sup>, F. Cicogna<sup>4</sup>, G.**  
15  
16 **Filippone<sup>5</sup>**  
17  
18  
19  
20  
21

22  
23 <sup>(1)</sup> Dipartimento di Ingegneria Civile, Ambientale, Aerospaziale, dei Materiali, Università di  
24  
25 Palermo, Viale delle Scienze, Ed. 6, 90128 Palermo, Italy

26  
27 <sup>(2)</sup> Department of Chemistry, Materials and Chemical Engineering "Giulio Natta", Politecnico  
28  
29 di Milano, Piazza Leonardo da Vinci, 32 - 20133 Milano, Italy

30  
31 <sup>(3)</sup> CNR-IPCB-Section of Catania, Via P. Gaifami, 18 -95126 Catania, Italy

32  
33  
34 <sup>(4)</sup> Istituto di Chimica dei Composti Organo Metallici (ICCOM), Consiglio Nazionale delle  
35  
36 Ricerche, UOS Pisa, Via G. Moruzzi 1, 56124 Pisa, Italy.

37  
38  
39 <sup>(5)</sup> Dipartimento di Ingegneria Chimica, dei Materiali e della Produzione Industriale, Università  
40  
41 di Napoli Federico II, Piazzale V. Tecchio, 80, 80125 Napoli, Italy  
42  
43  
44  
45  
46  
47  
48  
49  
50  
51  
52  
53  
54  
55  
56  
57

58  
59 

---

<sup>\*</sup> Corresponding author. Tel: +39 091 23863704. Fax: +39 091 23860841. E-mail address: nadka.dintcheva@unipa.it (N.Tz.  
60 Dintcheva).  
61  
62  
63  
64  
65

1           **Abstract**  
2  
3

4           Hindered Amine Light Stabilizer (HAS) molecules were covalently linked onto outer surface of  
5  
6           multi-walled carbon nanotubes (CNTs) and the obtained multi-functional fillers (HAS-*f*-CNTs)  
7  
8           were dispersed in Ultra High Molecular Weight Polyethylene (UHMWPE) aiming at obtaining  
9  
10          advanced nanocomposites with enhanced photo-oxidative stability, electrical and mechanical  
11  
12          properties. The effective grafting of HAS molecules is confirmed by spectroscopic,  
13  
14          spectrometric and thermo-gravimetric analyses, and the influence of the multi-functional  
15  
16          nanoparticles on the morphology, mechanical and electric behaviour and photo-oxidative  
17  
18          stability of the nanocomposites are investigated. UHMWPE/HAS-*f*-CNTs nanocomposite shows  
19  
20          improved electrical and mechanical properties compared with those of bare CNTs based  
21  
22          nanocomposites and, due to the multi-functional nature of used nanoparticles, shows enhanced  
23  
24          photo-oxidative stability caused by a synergic action between the immobilized HAS molecules  
25  
26          and the radical scavenging activity of CNTs.  
27  
28  
29  
30

31  
32  
33  
34           **Keywords:** A. Polymer-matrix composites (PMCs) A. Nano-structures B. Physical properties  
35  
36           B. Rheological properties B. Mechanical properties  
37  
38  
39  
40  
41  
42  
43  
44  
45  
46  
47  
48  
49  
50  
51  
52  
53  
54  
55  
56  
57  
58  
59  
60  
61  
62  
63  
64  
65

## 1. Introduction

The development of innovative multi-functional hybrid carbon-based nanoparticles and their polymer nanocomposites have gained a great interest among researchers in the last two decades [1-3]. One of the most promising candidates for the design of novel multi-functional nanoparticles and novel high performance polymer-based composites are the carbon nanotubes [4-5]. Particularly, the carbon nanotubes can be used as nanoparticles able to improve the electrical, thermal, mechanical and optical properties of the host matrix [6-7]. The chemical functionalization of CNTs, that can be achieved through *i*) covalent linkage [6], *ii*) non-covalent supramolecular absorption [7], *iii*) defect functionalization [8], or *iv*) modification through click chemistry [9], besides improving their dispersibility inside polymer matrices [10-12], provides them new functionalities enlarging their possible fields of application [13-14]. Thus CNTs can be used as substrate to graft functional groups having specific functionalities and they can be successfully considered as nano-carriers of the grafted moiety allowing, once dispersed in a polymer matrix, to combine all the structural advantages of this 1D nanofiller with the specific properties of the functional groups. In this work, hindered amine light stabilizers HAS molecules have been anchored onto outer surface of CNTs and the obtained multi-functional fillers (HAS-*f*-CNTs) have been used for the formulation of advanced Ultra High Molecular Weight Polyethylene (UHMWPE) nanocomposites. As well know, HAS are able to absorb the UV-light ensuring long-term stability of the host matrix [15]. A recent study by Lonkar [16] evidenced that MWCNTs modified with HALS dispersed in polypropylene matrix are able both to increase the induction period of PP photo-oxidation and to improve the mechanical properties of the nanocomposites. In the specific case of UHMWPE, and particularly in the radiation cross-linked material used in the design of artificial joints, HAS molecules have been suggested as possible stabilizers in place of the currently used Vitamin E (VE) [17]. HAS were proved to have better performances than VE due to the different stabilization mechanisms of the two classes of stabilizers. VE can react with alkyl radicals also during the radiation cross-linking of UHMWPE leading to a reduction of radiation efficiency or

1 cross-link density, this reaction caused also a lost of VE that was no more available during the  
2 use of the cross-linked material. HAS do not interfere with the cross-linking mechanism  
3 because they are added to the matrix in a non radical form, only after irradiation and in the  
4 presence of oxygen species HAS can be activated giving rise to a nitroxide able to react with  
5 radical species. Moreover, after the first step, the nitroxide can be regenerated according to the  
6 accepted radical scavenger mechanism of HAS [15]. As far as the preparation and use of  
7 CNTs/UHMWPE composites, they were reported in the literature also as possible alternative to,  
8 or as filler in, the radiation cross-linked material in the arthroplastic applications [18]. However,  
9 some concerns exist about the effective reinforcing ability of CNTs in the CNTs/UHMWPE  
10 composites because, due to the high viscosity of the matrix, the composites were generally  
11 prepared by solution or dry blending of CNTs with powdered UHMWPE followed by hot  
12 compaction. This procedure gives rise to composites having segregated structure instead of a  
13 random distribution and the segregated structure can introduce defects on the microstructure of  
14 UHMWPE that can negatively influence the mechanical properties of the material. To partially  
15 overcome this problem, chemical modification of CNTs with different functional groups was  
16 used to enhance the interactions between the filler and the polymer matrix giving good results  
17 both in terms of mechanical reinforcement of the matrix and by increasing also the stability of  
18 the composites because of the antioxidant effect of CNTs that limits the degradation of the  
19 material after long post-irradiation period. Indeed, according to the current literature, the CNTs  
20 exert a radical scavenging activity against oxidation of the polymer-based nanocomposites [19-  
21 20] and slightly UV-protective action during manufacture lifetime [21-22]. The radical  
22 scavenging activity of CNTs can be exacerbated through introduction of specific anti-oxidant  
23 functionalities [23] or UV-stabilizers [16] onto outer surface or immobilization of natural  
24 hindered phenols and/or polyphenols as experimentally demonstrated [24-25]. Meanwhile, the  
25 segregate structure of CNTs/UHMWPE composites has also the specific feature to allow the  
26 preparation of conductive material characterized by ultralow percolation threshold that probably  
27 can be further reduced by improving the dispersion of CNTs [26]. In this work, the preparation

1 and properties of UHMWPE/HAS-*f*-CNTs nanocomposites having enhanced photo-oxidative  
2 stability and durability were reported. Besides, due to the multi-functional nature of used  
3 nanofillers, the UHMWPE/nanocomposite show improved electrical and mechanical properties  
4 compared with those of bare CNTs based nanocomposites.  
5  
6  
7  
8  
9

## 10 11 12 13 14 **2. Experimental Part** 15

### 16 17 18 19 *2.1 Materials* 20

21 The UHMWPE is a commercial grade purchased by Sigma-Aldrich in the form of a white  
22 powder. Its main properties are: average molecular weight  $M_w=3\div 6$  MDa, softening point  
23  $T=136^\circ\text{C}$  (Vicat, ASTM D 1525B), melting point  $T_m=138^\circ\text{C}$  and density  $\rho=0.94$  g/mL at  $25^\circ\text{C}$ .  
24  
25 CNTs bearing hindered amine light stabilizer molecules (HAS) grafted on the outer surface  
26 (HAS-*f*-CNTs) were produced starting from multiwalled CNTs containing  $\sim 1$  wt.% of  
27 covalently linked -COOH groups (CNTs-COOH) purchased by Cheap Tubes, U.S.A. Their  
28 main features are: outer diameter  $OD=120\div 180$  nm, inner diameter  $ID=10\div 20$  nm, length  
29  $L=10\div 20$   $\mu\text{m}$ , purity  $>95$  wt.%, ash  $<1.5$  wt.%, specific surface area  $SSA>60$   $\text{m}^2/\text{g}$  and electrical  
30 conductivity  $EC>10^{-2}$  S/cm. Bare multiwalled CNTs were used to produce reference samples.  
31 They have  $OD=120\div 180$  nm,  $ID=10\div 20$  nm,  $L=10\div 20$   $\mu\text{m}$ , purity  $>95$  wt.%, ash  $<1.5$  wt.%,  
32  $SSA>40$   $\text{m}^2/\text{g}$  and  $EC>10^{-2}$  S/cm.  
33  
34  
35  
36  
37  
38  
39  
40  
41  
42  
43  
44

45 N,N'-dicyclohexylcarbodiimide (DCC) and 2,2,6,6-tetramethyl-4-piperidinol (light stabilizer  
46 molecules, HAS) were purchased from Sigma-Aldrich and utilized without further purifications.  
47  
48  
49  
50  
51

### 52 53 *2.2 Side-wall functionalized CNTs-COOH* 54

55 The covalent linkage between the side-wall carboxylic function of the CNTs (1) and the  
56 piperidinol (3) was obtained by esterification in the presence of DCC (see Figure 1). Due to  
57  
58  
59  
60  
61  
62  
63  
64  
65

1 steric hindrances, the endocyclic amino function of 2,2,6,6-tetramethyl-4-piperidinol is rather  
2 inert in the reaction conditions, and only the hydroxyl group is involved in the esterification.  
3  
4  
5 0.2 g of CNTs (1) were dispersed in a solution of 2,2,6,6-tetramethyl-4-piperidinol (3) (0.64  
6 mmol, 0.10 g) and DCC (0.19 mmol, 0.040 g) in 30 mL of dry THF. The resulting mixture was  
7  
8  
9  
10 sonicated in an ultrasound bath (240 W, 2.5 Lt) for 1 min then stirred at ambient temperature  
11  
12 under nitrogen atmosphere for 96 hours. After that time, the suspension was filtered on a  
13  
14 sintered glass filter, the CNTs were deeply washed many times with hot N,N'-  
15  
16 dimethylformamide and methanol, and dried at 90 °C overnight.  
17  
18  
19  
20

### 21 *2.3 Nanocomposite preparation*

22  
23 UHMWPE-based nanocomposites containing 1 wt% of bare CNTs, CNTs-COOH or HAS-f-  
24  
25 CNTs were prepared by hot compaction (HC) using a hydraulic Carver press. Polymer and  
26  
27 CNTs were manually mixed at room temperature to obtain a homogeneous black powder, which  
28  
29 was loaded between the plates of the press and compressed at a pressure  $P=1500$  psi for 5 min at  
30  
31 temperature  $T=210^{\circ}\text{C}$ . The resulting thin films (thickness  $\sim 80$   $\mu\text{m}$ ) were used for the subsequent  
32  
33 analyses. Pure UHMWPE and UHMWPE/HAS thin films prepared by HC were used as  
34  
35 reference samples.  
36  
37  
38  
39  
40

### 41 *2.4 Characterization*

42  
43 ATR-FTIR analysis of CNTs-COOH and HAS-f-CNTs was performed using a Fourier  
44  
45 Transform Infrared Spectrometer (FTIR) (Spectrum Two FTIR spectrometer, Perkin Elmer)  
46  
47 equipped with a diamond crystal for surface analysis. Spectra collected on three different  
48  
49 batches of each sample (milligram level) were obtained by accumulation of 32 scans between  
50  
51 4000 and 1000  $\text{cm}^{-1}$ , with a resolution of 4  $\text{cm}^{-1}$ .  
52  
53  
54 Fourier transform infrared spectroscopy (FT-IR) of polymer films was carried out by using a  
55  
56 Perkin Elmer FT-IR spectrometer (mod. Spectrum Two). The spectra were collected by  
57  
58 performing 16 scans between 4000 and 500  $\text{cm}^{-1}$ .  
59  
60  
61  
62  
63  
64  
65

1 Thermogravimetric analyses (TGA) were carried out on the bare and functionalized CNTs by  
2  
3 using an Exstar TG/DTA Seiko 7200 instrument. The tests were performed at a heating rate of  
4  
5 10°C/min from 30 to 750°C under nitrogen flow. The reported results are the average of three  
6  
7 independent measurements on batches of ~5 mg. The standard deviation was ±0.3% for each  
8  
9 investigated sample.

10  
11 Micro-Raman spectroscopy has been performed at room temperature through a Bruker-Senterra  
12  
13 micro-Raman equipped with a 532 nm diode laser excitation and 20 mW power. Non-confocal  
14  
15 measurements were carried out in the range 4000–400 cm<sup>-1</sup> with a spectral resolution between 9  
16  
17 and 15 cm<sup>-1</sup>.

18  
19 The Py-GCMS experiments were carried out on a Frontier Laboratories' Multi-Shot Pyrolyzer  
20  
21 EGA/PY-3030D with direct connection to a Shimadzu GCMS-TQ8040 gas chromatography  
22  
23 mass spectrometer (GC-MS) equipped with a 30 m × 0.25 mm inner diameter (5%-phenyl)-  
24  
25 methylpolysiloxanenon-polar column (HP5MS). The pyrolyzer was set at 350°C to a final of  
26  
27 experiment. The GC/MS conditions were the following: inlet temperature at 250°C, pressure 7.1  
28  
29 psi, split ratio 50:1. The oven temperature of the GC was held at 40°C for 1 min followed by  
30  
31 continuous heating (6°C/min) to 280°C with 1 mL/min helium carrier gas. Then, the final  
32  
33 temperature was held for 15 min to ensure that no heavy molecules remained in the column. The  
34  
35 mass spectrometer conditions used were: transfer line temperature 150°C, ion source  
36  
37 temperature 230°C, and electron impact ionization (EI) at 70 eV.

38  
39 Rheological tests were performed using a strain-controlled rheometer (mod. ARES G2 by TA  
40  
41 Instrument) in parallel plate geometry (plate diameter 25 mm). The complex viscosity ( $\eta^*$ ) was  
42  
43 measured performing frequency scans from  $\omega=10^{-1}$  to  $10^2$  rad/s at  $T=210^\circ\text{C}$ . The strain  
44  
45 amplitude was  $\gamma=2\%$ , which preliminary strain sweep experiments proved to be low enough to  
46  
47 be in the linear viscoelastic regime.

48  
49 Optical microscopy was performed using a Leica Microscope in reflection mode at a  
50  
51 magnification of 20x. Images were acquired on the surface of the nanocomposite films.  
52  
53  
54  
55  
56  
57  
58  
59  
60  
61  
62  
63  
64  
65

1 Electrical resistivity of each film was measured employing a commercial setup (ECOPIA HMS-  
2  
3 3000, B=0.55 T) at room temperature.  
4

5 Dynamic Mechanical Thermal Analysis (DMTA) was performed using a Rheometrics DMTA V  
6  
7 instrument, single cantilever bending method. The test has been carried out in the temperature  
8  
9 swift mode, between 10 and 120°C at a heating rate of 2 °C/min. The frequency was set to 1 Hz  
10  
11 and the maximum strain amplitude was 0.5%. The elastic modulus ( $E'$ ) as a function of the  
12  
13 temperature was recorded.  
14  
15

16 Photo-oxidation of polymer films was carried out using a Q-UV weatherometer equipped with  
17  
18 UVB lamps (313 nm). The progress of the photo-degradation was quantified by referring to the  
19  
20 carbonyl (CI) and hydroxyl (HI) indices as a function of irradiation time. CI was calculated as  
21  
22 the ratio between the integral of the carbonyl absorption region (1850-1600  $\text{cm}^{-1}$ ) and that of a  
23  
24 reference peak at about 1370  $\text{cm}^{-1}$ ; HI refers to the hydroxyl absorption region (3570–3150  $\text{cm}^{-1}$ ),  
25  
26 which integral was normalized by the peak at 1370  $\text{cm}^{-1}$ .  
27  
28  
29  
30  
31  
32  
33

### 34 **3. Results and Discussion**

#### 35 *3.1 Characterization of HAS-f-CNTs*

36  
37  
38  
39  
40  
41 Reactive hindered amine light stabilizer molecules were successfully grafted onto the outer  
42  
43 surface of the CNTs-COOH (see Figure 1) and the surface functionalization was assessed  
44  
45 through ATR-FTIR, Raman spectroscopy, TGA and mass spectrometry. In Figure 2, the ATR-  
46  
47 FTIR spectra of CNTs-COOH and HAS-f-CNTs are shown. The spectra of HAS-f-CNTs  
48  
49 displays a strong absorption band at 2966  $\text{cm}^{-1}$  and a broad absorption band centred at around  
50  
51 2852  $\text{cm}^{-1}$  due to the asymmetrical ( $\nu_{\text{as}}\text{CH}_3$ ) and symmetrical ( $\nu_{\text{s}}\text{CH}_3$ ) stretching of C-H bonds in  
52  
53 methyl groups, respectively. Besides, a broad absorption band centred at around 3100  $\text{cm}^{-1}$   
54  
55 possibly due to N-H stretching vibration of the grafted functional group, is also visible.  
56  
57  
58  
59  
60  
61  
62  
63  
64  
65

1 Additionally, the TGA analysis suggest that both the CNTs-COOH and HAS-*f*-CNTs  
2 decompose faster than the bare CNTs with increasing the temperature, because of the  
3 volatilization of carboxyl and HAS molecules on the nanotube surface. The gradual weight loss  
4 related to the thermal decomposition of the HAS groups takes place in the range 300÷400°C,  
5 i.e. well above the temperature at which the nanocomposite thin films were prepared and  
6 characterized. Probably, the weight loss up to 100 °C is due to a small amount of residual water  
7 in all the samples. The residues at the end of the analysis were 98.1% wt and 96.0% wt for  
8 CNTs-COOH and HAS-*f*-CNTs, respectively, whereas a residual of 99.1% wt was found for the  
9 bare CNTs due to a partial decomposition of the bulk material, see Figure 3. Moreover, TGA  
10 revealed an overall content of HAS around 2.0 wt.% (see Figure 3).

11 The surface functionalization of CNT with HAS already evidenced by ATR-FTIR and TGA  
12 analysis, was further confirmed by the GC-MS analysis of pyrolyzed HAS-*f*-CNT obtained.  
13 Particularly, in Figure 4, (a) an enlargement portion of GC signal assigned to 2,2,6,6-  
14 tetramethyl-4-piperidinol in Py-GC MS and (b) corresponding mass spectrum matched with (c)  
15 database mass spectrum of 2,2,6,6-tetramethyl-4-piperidinol are shown, respectively. Almost  
16 total matching between the MS spectra of our sample (see spectra b) and database mass spectra  
17 (see spectra c) can be observed suggesting the presence of 2,2,6,6-tetramethyl-4-piperidinol.  
18 Finally, according to our previous study [24], CNTs lattice defect due to the functionalization  
19 can be detected by the Raman spectroscopy by considering the ratio between the signal  
20 intensities of the disorder-induced D-band at  $\sim 1340\text{ cm}^{-1}$  ( $I_D$ ) and tangential G-band at  $\sim 1570$   
21  $\text{cm}^{-1}$  ( $I_G$ ) [27-28]. The Raman spectra of bare CNTs, CNTs-COOH and HAS-*f*-CNTs sample are  
22 compared in Figure 5.

23 The  $I_D/I_G$  ratio of bare CNTs is about 0.47, while it increases significantly for both CNTs-  
24 COOH ( $I_D/I_G = 1.12$ ) and HAS-*f*-CNTs ( $I_D/I_G = 1.40$ ) samples, suggesting that the presence of  
25 carboxylic groups, and even more HAS, allows for the formation of a large amount of surface  
26 defects. Furthermore, a slight shift of tangential G-band for HAS-*f*-CNTs compared to the bare  
27 CNTs and intensification of the shoulder centred at around  $1605\text{ cm}^{-1}$  are due to the

1 modification occurring in the structure of CNTs suggesting successful grafting of HAS, also  
2  
3 according to the literature [28].  
4  
5  
6

### 7 *3.2 Characterization of UHMWPE-based nanocomposites*

8  
9 As well known, the molecular architecture changes in polymers and polymer-based  
10  
11 nanocomposites may be gainfully investigated through rheology analysis. Additionally, the  
12  
13 rheological analysis of nano-filled polymers provides valuable information in terms of the state  
14  
15 of nanoparticles dispersion. The complex viscosity curves ( $\eta^*$ ) and elastic ( $G'$ ) and loss ( $G''$ )  
16  
17 moduli of neat UHMWPE and investigated nanocomposites as a function of frequency are  
18  
19 shown in Figure 6 (a-b). First we evaluate the effect of the HAS presence on the rheological  
20  
21 behaviour of UHMWPE. The complex viscosity and both moduli of UHMWPE/HAS are  
22  
23 slightly lower than those of neat UHMWPE because of a plasticizing effect exerted by HAS.  
24  
25 Indeed these low molecular weight compounds can diffuse within the molten polymer causing  
26  
27 the decrease of the matrix viscosity through an increase of the free volume, by increasing the  
28  
29 space between macromolecules and sometimes facilitating their slipping. Concerning the effect  
30  
31 of the nanotubes addition, the  $\eta^*$  values of all nanocomposites are higher than those of neat  
32  
33 UHMWPE in the whole investigated frequency range. The bare CNTs have an irrelevant effect,  
34  
35 resulting in a mere vertical shift of the  $\eta^*$  curve, without actually altering the relaxation  
36  
37 spectrum of matrix macromolecules. This feature is typical of not uniformly dispersed fillers.  
38  
39 Differently, CNTs-COOH and especially HAS-*f*-CNTs are able to generate noticeable  
40  
41 rheological alterations; the disappearance of Newtonian plateau for HAS-*f*-CNTs containing  
42  
43 nanocomposites suggests their arrangement in interconnected structures, resulting in the  
44  
45 formation of a semi-3D network of nanoparticles into the host matrix. Consistent with the  
46  
47 addition of solid particles into a polymer matrix,  $G'$  and  $G''$  of UHMWPE-based  
48  
49 nanocomposites increases at all frequencies with the nanoparticles adding, following the same  
50  
51 trend observed for the viscosity. Nevertheless, alterations in the low frequency behaviour  
52  
53 emerge, and the low frequency  $G'$  modulus of functionalized CNTs containing nanocomposites  
54  
55  
56  
57  
58  
59  
60  
61  
62  
63  
64  
65

1 tends to become almost independent of frequency, suggesting a pseudo solid-like behaviour.

2  
3 Once again, this issue is more pronounced for nanocomposite containing HAS-*f*-CNTs.

4  
5 The visual inspections of the nanocomposite films agree with the indications emerged from the  
6  
7 rheological analysis. Representative optical micrographs of the UHMWPE-based

8  
9 nanocomposites containing bare CNTs, CNTs-COOH and HAS-*f*-CNTs are shown in Figure 7.

10  
11 The CNTs appear as the dark phase. The optical observations show that a segregated structure,  
12  
13 in which CNTs are mainly localized in the interfacial regions of UHMWPE particles, has been  
14  
15 successfully achieved in all UHMWPE-based nanocomposites. In fact, when “hot-compaction”  
16  
17 method is used for the nanocomposites preparation, the nanotubes cover the surface of the  
18  
19 polymer particles in powdered UHMWPE/nanoparticles mixture, and after hot pressing the  
20  
21 nanoparticles remain at boundaries between the polymer particles. As a result the formation of  
22  
23 CNTs-rich channels around UHMWPE-rich islands can be achieved [18]. Comparison between  
24  
25 the morphology of bare and functionalized-CNTs based nanocomposites indicates that in the  
26  
27 former a broader segregated networks within host matrix has been obtained, probably due to  
28  
29 some re-aggregation phenomena between CNTs that hinder their distribution in the interfacial  
30  
31 regions. The presence of COOH and HAS functional groups in functionalized-CNTs based  
32  
33 nanocomposites, avoid the CNTs agglomeration, allowing the formation of a well-ordered  
34  
35 segregated structure.  
36  
37  
38  
39

40  
41 These segregated networks are beneficial to form conductive nanoparticles paths through the  
42  
43 host matrix. The electrical resistivity of neat UHMWPE and CNTs containing nanocomposites  
44  
45 with segregated morphology has been measured at least three times for each sample and the  
46  
47 average values were calculated and reported in Table 1. As expected the unfilled UHMWPE  
48  
49 shows highest values of resistivity and the addition of bare CNTs causes a variation of the  
50  
51 resistivity value by two orders of magnitude. Even more, by adding of CNTs-COOH and HAS-  
52  
53 *f*-CNTs, the values of the resistivity change by three orders of magnitude suggesting a beneficial  
54  
55 effect of the presence of both COOH and HAS functional groups in the nanotubes dispersion  
56  
57 and formation of segregated morphology, as reported above. It is interesting to highlight that the  
58  
59  
60  
61  
62  
63  
64  
65

1 presence of HAS moiety onto CNTs outer surface does not affect negatively the formation of  
2  
3 the conductive channels around UHMWPE-rich islands highlighting the possibility to use HAS-  
4  
5 *f*-CNTs as multi-functional fillers for the formulation of advanced innovative polymer-based  
6  
7 nanocomposites.  
8

9  
10 To investigate the mechanical behaviour of the nanocomposites, the elastic modulus ( $E'$ ) as a  
11  
12 function of the temperatures for neat UHMWPE and all nanocomposites has been monitored  
13  
14 and the trends are shown in Figure 8; the insert reports the values of the  $E'$  at two different  
15  
16 temperatures. As expected the  $E'$  decreases with temperature increase for all investigated  
17  
18 samples and this effect is more pronounced for the neat UHMWPE and UHMWPE/HAS  
19  
20 samples. The presence of free HAS molecules causes a slight decrease of the elastic modulus  
21  
22 value, confirming the plasticizing action of the HAS molecules noticed by rheological  
23  
24 investigations.  
25  
26

27  
28 The CNTs-containing samples show less pronounced temperature dependence and higher  $E'$   
29  
30 values than that of neat UHMWPE. All used CNTs exert reinforcement action for UHMWPE  
31  
32 matrix and this effect is more pronounced for the functionalized CNTs. The obtained segregate  
33  
34 morphology, discussed before, for CNTs-containing samples could be considered responsible  
35  
36 for the mechanical behaviour.  
37  
38  
39  
40

### 41 *3.3 Photo-oxidation behaviour of UHMWPE-based nanocomposites*

42

43 To investigate the photo-oxidation behaviour of UHMWPE-based nanocomposites, thin films  
44  
45 have been subjected to accelerate UVB exposure and the formation of carbonyl and hydroxyl  
46  
47 species as a function of the exposure time has been monitored through FTIR analysis. In Figure  
48  
49 9 (a-b), the calculated carbonyl (CI) and hydroxyl (HI) indices of investigated neat UHMWPE,  
50  
51 UHMWPE/HAS and UHMWPE-based nanocomposites are shown. The CI refers to the signals  
52  
53 in the range  $1850$  to  $1600\text{ cm}^{-1}$ , which are due to the formation of different amount of carbonyl  
54  
55 species and reflect the formation of acid ( $1715\text{ cm}^{-1}$ ), ketones ( $1718\text{ cm}^{-1}$ ), esters ( $1738\text{ cm}^{-1}$ )  
56  
57 and lactones ( $1786\text{ cm}^{-1}$ ). The HI is related to the presence of linked and free -OH groups  
58  
59  
60  
61  
62  
63  
64  
65

1 deriving from the photo-oxidation process. Concerning the CNTs and CNTs-COOH based  
2 nanocomposites, the nanotubes are able to protect or slightly slow down, the photo-oxidation of  
3 UHMWPE [21]. Indeed CNTs are able to exert a radical scavenging activity because of the  
4 presence of surface defects that causes the formation of acceptor-like localized states and this  
5 future significantly improve the radical scavenging activity of the carbon nanotubes [19-20].  
6 Moreover, CNTs can also act as inner filter, decreasing the rate at which the polymer matrix is  
7 oxidized [29]. Furthermore, the CNTs upon UV light are able to physisorb the oxygen  
8 molecules which, being strongly bonded on the walls of carbon nanotubes, are not available for  
9 the oxidative phenomena [22]. All these features can explain the observed slight protection  
10 activity of CNTs and CNTs-COOH against UVB light in the UHMWPE/CNT composites  
11 which is more pronounced for CNTs-COOH characterized by a large amount of structural  
12 defects as confirmed by Raman analysis. The dispersed HAS molecules in UHMWPE are able  
13 to protect the UHMWPE against the UVB exposure for longer time with respect to pristine  
14 polymer or CNT/UHMWPE composites, however its low molecular weight could be considered  
15 responsible for volatilization during processing and subsequent reduced protection action. The  
16 protective activity of both CNTs or HAS is further increased by the presence of HAS molecules  
17 covalently linked onto their outer surface. In fact, UHMWPE/HAS-f-CNTs show best photo-  
18 oxidation resistance, in terms of delayed induction time (time at which the slope of the carbonyl  
19 and hydroxyl indices curves change suddenly) and of decreased rate of oxygen containing  
20 species formation. The very high photo-oxidative resistance of UHMWPE/HAS-f-CNTs film  
21 can be understood considering different features. First of all, immobilized HAS molecules are  
22 not subjected to volatilization and/or migration so they can exert their stabilisation effect for a  
23 longer time. Moreover, they are localized and available at the interfacial area between  
24 polymeric phase and the inert nanofillers that is the critical area for the beginning of photo  
25 degradation process. Moreover, the chemical functionalization (shown in Figure 1) induces the  
26 formation of sidewall defects, as confirmed by Raman analysis, which act as acceptor-like  
27  
28  
29  
30  
31  
32  
33  
34  
35  
36  
37  
38  
39  
40  
41  
42  
43  
44  
45  
46  
47  
48  
49  
50  
51  
52  
53  
54  
55  
56  
57  
58  
59  
60  
61  
62  
63  
64  
65

1 localised states conferring an additional free-radical scavenging activity to the nanoparticles, as  
2  
3 recently documented by experimental [19-20] and theoretical [30] studies.  
4  
5  
6  
7  
8  
9

#### 10 **4. Conclusions**

11  
12 Multi-functional filler based on CNTs bearing covalently linked HAS molecules has been  
13  
14 successfully obtained and its characterization has been performed through advanced  
15  
16 spectroscopic, spectrometric and thermo-gravimetric analysis. Besides, the HAS-*f*-CNTs has  
17  
18 been incorporated into UHMWPE for the formulation of advanced nanocomposite, whose  
19  
20 properties and performance have been compared with those of bare CNTs and CNTs-COOH  
21  
22 based nanocomposites. The UHMWPE/HAS-*f*-CNTs nanocomposite shows enhanced photo-  
23  
24 oxidative stability, electrical and mechanical properties due to the multi-functional nature of the  
25  
26 successfully formulated nanofiller.  
27  
28  
29  
30  
31  
32  
33  
34

35 **Acknowledgements:** this work has been financially supported by Ministry of University and  
36  
37 Research in Italy (MIUR), FIRB2010 – Futuro in Ricerca, Project title: "GREENER – Towards  
38  
39 multifunctional, efficient, safe and stable “green” bio-plastics based nanocomposites of  
40  
41 technological interest via the immobilization of functionalized nanoparticles and stabilizing  
42  
43 molecules" (cod: RBFR10DCS7).  
44  
45  
46  
47  
48  
49  
50  
51  
52  
53  
54  
55  
56  
57  
58  
59  
60  
61  
62  
63  
64  
65

## References

- [1] Noorden RV. The trials of new carbon. *Nature* 2011;469(7328):14-16.
- [2] Xu JZ, Zhong GJ, Hsiao BS, Fu O, Li ZM. Low-dimensional carbonaceous nanofiller induced polymer crystallization. *Prog Polym Sci* 2013;39(3):555-593.
- [3] Arrigo R, Dintcheva NT, Morici E, La Mantia FP. Performances and morphology of polyamide/carbonaceous structures based fibers. *AIP Proc* 2014;1599:330-333.
- [4] Spitalsky Z, Tasis D, Papagelis K, Galiotis C. Carbon nanotube–polymer composites: Chemistry, processing, mechanical and electrical properties. *Prog Polym Sci* 2010; 35(3): 357–401.
- [5] Dintcheva NT, Arrigo R, Morreale M, La Mantia FP, Matassa R, Caponetti E. Effect of elongational flow on morphology and properties of polymer/CNTs nanocomposite fibers. *Polym Adv Tech* 2011;22(12):1612-1619.
- [6] Dintcheva NT, Arrigo R, Nasillo G, Caponetti E, La Mantia FP. On the role of extensional flow in morphology and properties modifications in MW-CNTs polyamide-based fibres. *Macromol Mater Eng* 2011;296(7):645–657.
- [7] Dintcheva NT, Arrigo R, Nasillo G, Caponetti E, La Mantia FP. Effect of the Nanotube Aspect Ratio and Surface Functionalization on the Morphology and properties of Multiwalled Carbon Nanotube Polyamide-Based Fibers. *J Appl Polym Sci* 2013;129(2013):2479-2489.
- [6] Yang M, Gao Y, Li H, Adronov A. Functionalization of multiwalled carbon nanotubes with polyamide 6 by anionic ring-opening polymerization. *Carbon* 2007;45(12):2327-2333.
- [7] Nativ-Roth E, Shvartzman-Cohen R, Bounioux C, Florent M, Zhang D, Szleifer I, Yerushalmi-Rozenet R. Physical adsorption of block copolymers to SWNT and MWNT: a nonwrapping mechanism. *Macromolecules* 2007;40(10):3676-3685.
- [8] Mawhinney DB, Naumenko V, Kuznetsova A, Yates JT, Liu J, Smalley RE. Surface defect site density on single walled carbon nanotubes by titration. *Chem Phys Lett* 2000;324(1-3):213–216.

- 1 [9] Campidelli S, Ballesteros B, Filoramo A, Diaz DD, Torre G, Torres T, Aminur Rahman  
2 GM, Ehli C, Kiessling D, Werner F, Sgobba V, Guldi DM, Cioffi C, Prato M, Bourgojn JP.  
3 Facile decoration of functionalized single-wall carbon nanotubes with phthalocyanines via click  
4 chemistry. *J Am Chem Soc* 2008;130(34):11503–11509.  
5  
6  
7  
8  
9 [10] Roy N, Sengupta R, Bhowmick AK. Modifications of carbon for polymer composites and  
10 nanocomposites. *Prog Polym Sci* 2012;37(6):781–819.  
11  
12  
13 [11] Sahoo NG, Rana S, Cho JW, Li L, Chan SH. Polymer nanocomposites based on  
14 functionalized carbon nanotubes. *Prog Polym Sci* 2010;35(7):837–867.  
15  
16  
17 [12] Karousis N, Tagmatarchis N. Nanotubes. Current progress on the chemical modification of  
18 carbon. *Chem Rev* 2010;110(9):5366–5397.  
19  
20  
21 [13] Wang J, Yuan R, Chai Y, Cao S, Guan S, Fu P, Min L. A novel immunosensor based on  
22 gold nanoparticles and poly-(2,6-pyridinediamine)/multiwall carbon nanotubes composite for  
23 immunoassay of human chorionic gonadotrophin. *Biochem Eng J* 2010;51(3):95–101.  
24  
25  
26 [14] Chen RJ, Zhang Y, Wang D, Dai H. Noncovalent Sidewall Functionalization of Single-  
27 Walled Carbon Nanotubes for Protein Immobilization. *J Am Chem Soc* 2001;123(16):3838–  
28 3839.  
29  
30  
31 [15] Gensler R, Plummer CJG, Kausch HH, Kramer E, Pauquet JR, Zweifel H. Thermo-  
32 oxidative degradation of isotactic polypropylene at high temperatures: phenolic antioxidants  
33 versus HAS. *Polym Derg Stab* 2000;67:195-208.  
34  
35  
36 [16] Lonkar SP, Kushwaha OS, Leuteritz A, Heinrich G, Singh RP. Self photostabilizing UV-  
37 durable MWCNT/polymer nanocomposites. *RSC Adv* 2012;2 (32):12255-12262.  
38  
39  
40 [17] Gijisman P, Smelt HJ, Schumann, D. Hindered amine light stabilizers: An alternative for  
41 radiation cross-linked UHMwPE implants. *Biomaterials* 2010;31:6685-6691.  
42  
43  
44 [18] Puértolas JA, Kurtz SM. Evaluation of carbon nanotubes and graphene as reinforcements  
45 for UHMWPE-based composites in arthroplastic applications: A review *J Mech Behav Biomed*  
46 2014; 39:129-145.  
47  
48  
49  
50  
51  
52  
53  
54  
55  
56  
57  
58  
59  
60  
61  
62  
63  
64  
65

- 1 [19] Watts PCP, Fearon PK, Hsu WK, Billingham NC, Kroto HW, Walton DRM. Carbon  
2  
3 nanotubes as polymer antioxidants. *J Mater Chem* 2003;13:491–495.  
4
- 5 [20] Shi X, Jiang B, Wang J, Yang Y. Influence of wall number and surface functionalization of  
6  
7 carbon nanotubes on their antioxidant behaviour in high density polyethylene. *Carbon*  
8  
9 2012;50(3):1005-1013.  
10
- 11 [21] Dintcheva NT, La Mantia FP, Malatesta V. Photo-oxidation behaviour of  
12  
13 polyethylene/multi-wall carbon nanotube composite films. *Polym Degrad Stab* 2009;94(2):162–  
14  
15 170.  
16
- 17 [22] Guadagno L, Naddeo C, Raimondo M, Gorrasi G, Vittoria V. Effect of carbon nanotubes  
18  
19 on the photo-oxidative durability of syndiotactic polypropylene. *Polym Degrad Stab*  
20  
21 2010;95(9):1614–1626.  
22
- 23 [23] Conyers JL, Lucente-Schultz RM, Moore VC, Leonard AD, Price BK, Kosynkin DV, Lu  
24  
25 M, Partha R, Conyers JL, Tour JM. Antioxidant single-walled carbon nanotubes. *J Am Chem*  
26  
27 *Soc* 2009;131(11):3934–3941.  
28
- 29 [24] Dintcheva NT, Arrigo R, Gambarotti C, Carroccio S, Filippone G, Cicogna F, Guenzi M.  
30  
31  $\alpha$ -Tocopherol-induced radical scavenging activity in carbon nanotubes for thermo-oxidation  
32  
33 resistant ultra-high molecular weight polyethylene-based nanocomposites. *Carbon* 2014;74:14-  
34  
35 21.  
36
- 37 [25] Dintcheva NT, Arrigo R, Gambarotti C, Guenzi M, Carroccio S, Cicogna F, Filippone G.  
38  
39 Immobilization of natural anti-oxidants on carbon nanotubes and aging behavior of ultra-high  
40  
41 molecular weight polyethylene-based nanocomposites. *AIP Conf Proc* 2014;1599:102-105.  
42
- 43 [26] Lisunova MO, Mamunya YeP, Lebovka NI, Melezhyk AV. Percolation behaviour of  
44  
45 ultrahigh molecular weight polyethylene/multi-walled carbon nanotubes composites. *Eur Polym*  
46  
47 *J* 2007;43:949-958  
48
- 49 [27] Qian WZ, Liu T, Wei F, Yuan HY. Quantitative Raman characterization of the mixed  
50  
51 samples of the single and multi-walled carbon nanotubes. *Carbon* 2003;41: 1851-1854.  
52  
53  
54  
55  
56  
57  
58  
59  
60  
61  
62  
63  
64  
65

- 1 [28] Holzinger M, Abraham J, Whelan P, Graupner R, Ley L, Hennrich F, Kappes M, Hirsch A.  
2  
3 Functionalization of Single-Walled Carbon Nanotubes with (R-)Oxycarbonyl Nitrenes. *J Am*  
4  
5 *Chem Soc* 2003;125(28):8566–8580.  
6  
7 [29] Morlat-Therias S, Fanton E, Gardette JL, Peeterbroeck S, Alexandre M, Dubois P.  
8  
9 *Polymer/carbon nanotube nanocomposites: Influence of carbon nanotubes on EVA*  
10  
11 *photodegradation. Polym Degr Stab* 2007;92(10):1873-1882.  
12  
13 [30] Galano A. Carbon Nanotubes as Free-Radical Scavengers. *J Phys Chem C* 2008;112  
14  
15 (24):8922–8927.  
16  
17  
18  
19  
20  
21  
22  
23  
24  
25  
26  
27  
28  
29  
30  
31  
32  
33  
34  
35  
36  
37  
38  
39  
40  
41  
42  
43  
44  
45  
46  
47  
48  
49  
50  
51  
52  
53  
54  
55  
56  
57  
58  
59  
60  
61  
62  
63  
64  
65

1           **Captions for Table and Figure**  
2

3           **Table 1.** Electrical resistivity values for neat UHMWPE and all investigated nanocomposites  
4

5           **Figure 1.** Scheme of side-wall functionalization of CNTs by 2,2,6,6-tetramethyl-4-piperidinol  
6

7           **Figure 2.** ATR-FTIR spectra of CNTs-COOH and HAS-*f*-CNTs  
8

9           **Figure 3.** TGA curves of bare CNTs, CNTs-COOH and HAS-*f*-CNTs  
10

11           **Figure 4.** (a) An enlargement portion of Py-GC signal assigned to 2,2,6,6-tetramethyl-4-  
12 piperidinol in Py-GC MS and (b) corresponding mass spectrum matched with (c) database mass  
13 spectrum of 2,2,6,6-tetramethyl-4-piperidinol  
14  
15  
16  
17

18           **Figure 5.** Raman spectra of bare CNTs, CNTs-COOH and HAS-*f*-CNTs  
19

20           **Figure 6.** (a) Complex viscosity curves ( $\eta^*$ ) and (b) elastic ( $G'$ ) and loss ( $G''$ ) moduli of neat  
21 UHMWPE and investigated nanocomposites  
22  
23

24           **Figure 7.** Optical micrographs of all investigated UIHMWPE-based nanocomposites  
25

26           **Figure 8.** Elastic modulus  $E'$  as a function of temperature for all investigated systems  
27

28           **Figure 9.** Carbonyl (a) and hydroxyl (b) indices as a function of the photo-oxidation time for  
29 all investigated systems  
30  
31  
32  
33  
34  
35  
36  
37  
38  
39  
40  
41  
42  
43  
44  
45  
46  
47  
48  
49  
50  
51  
52  
53  
54  
55  
56  
57  
58  
59  
60  
61  
62  
63  
64  
65

	$\rho$ [ $\Omega \cdot m$ ]
<b>UHMWPE</b>	$1.1 \cdot 10^8$
<b>UHMWPE/CNTs</b>	$1.6 \cdot 10^6$
<b>UHMWPE/COOH-CNTs</b>	$7.7 \cdot 10^5$
<b>UHMWPE/HAS-<i>f</i>-CNTs</b>	$5.2 \cdot 10^5$

**Table 1.** Electrical resistivity values for neat UHMWPE and all investigated nanocomposites

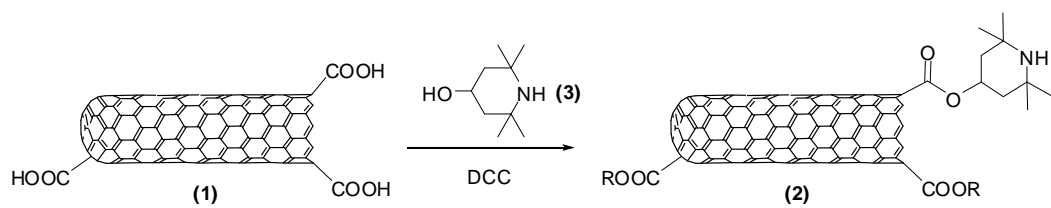


**Figure 1.** Scheme of side-wall functionalization of CNTs by 2,2,6,6-tetramethyl-4-piperidinol

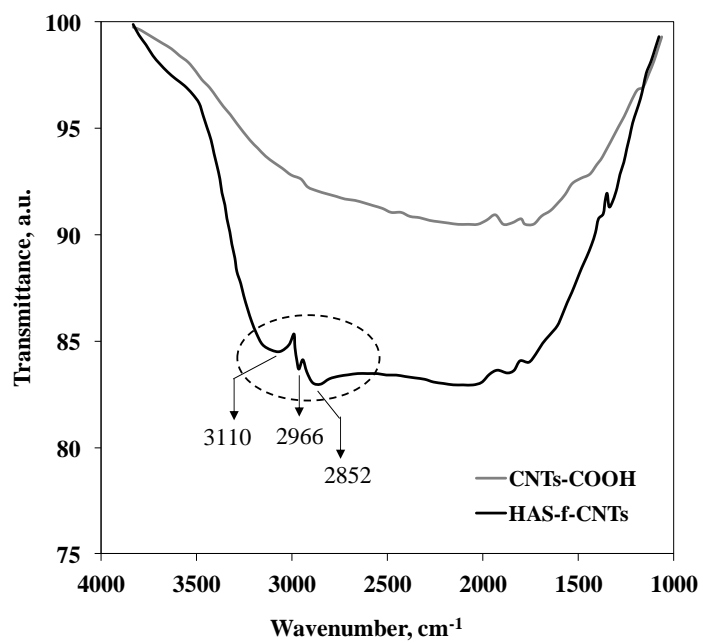


**Figure 2.** ATR-FTIR spectra of CNTs-COOH and HAS-*f*-CNTs

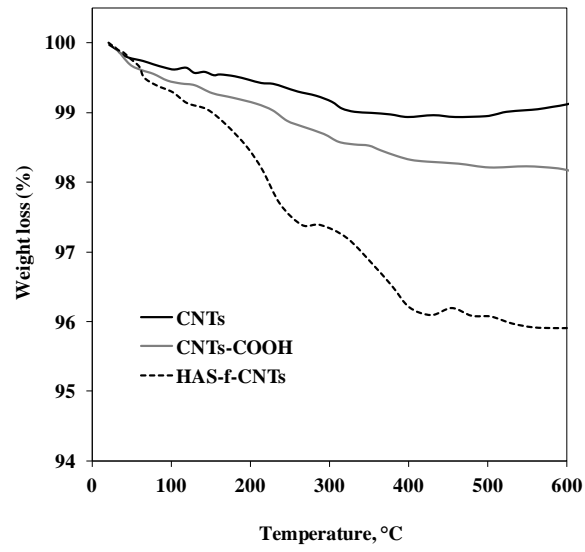
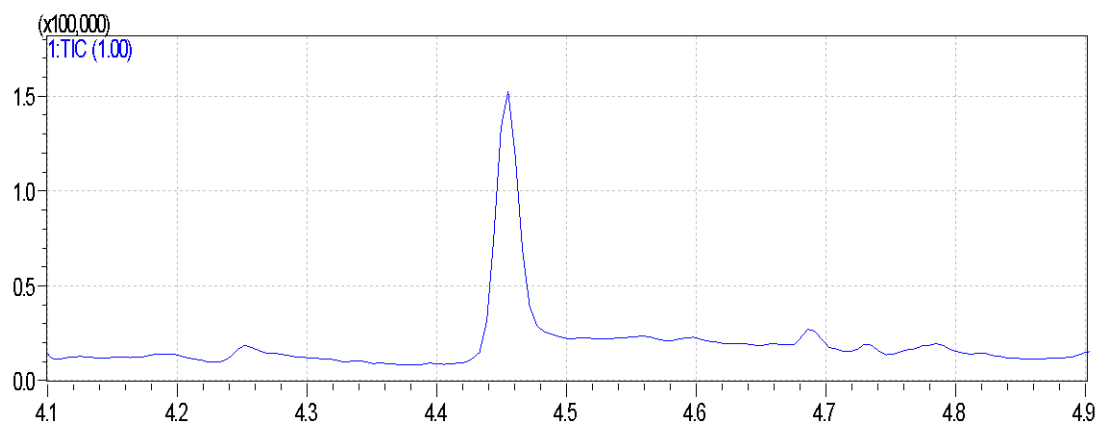
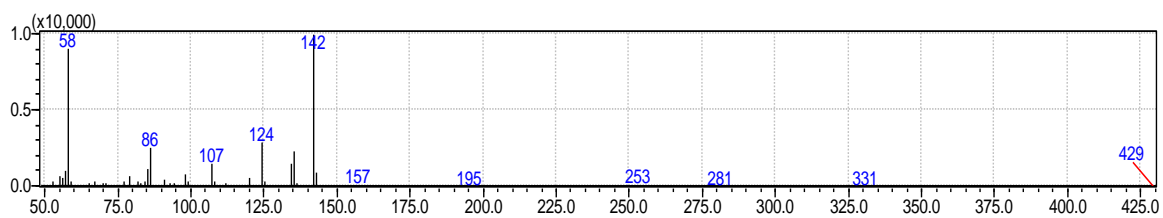


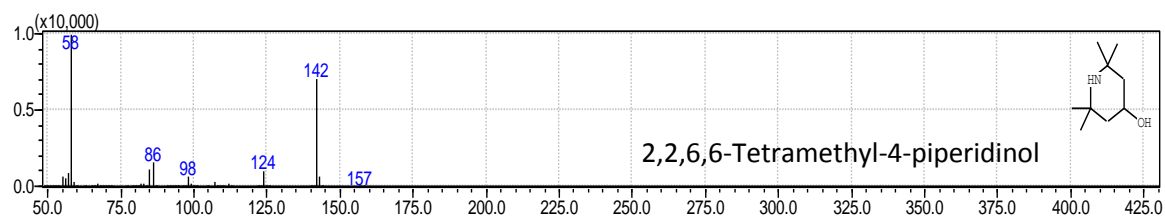
**Figure 3.** TGA curves of bare CNTs, CNTs-COOH and HAS-*f*-CNTs



(a)



(b)



(c)

**Figure 4.** (a) An enlargement portion of Py-GC signal assigned to 2,2,6,6-tetramethyl-4-piperidinol in Py-GC MS and (b) corresponding mass spectrum matched with (c) database mass spectrum of 2,2,6,6-tetramethyl-4-piperidinol

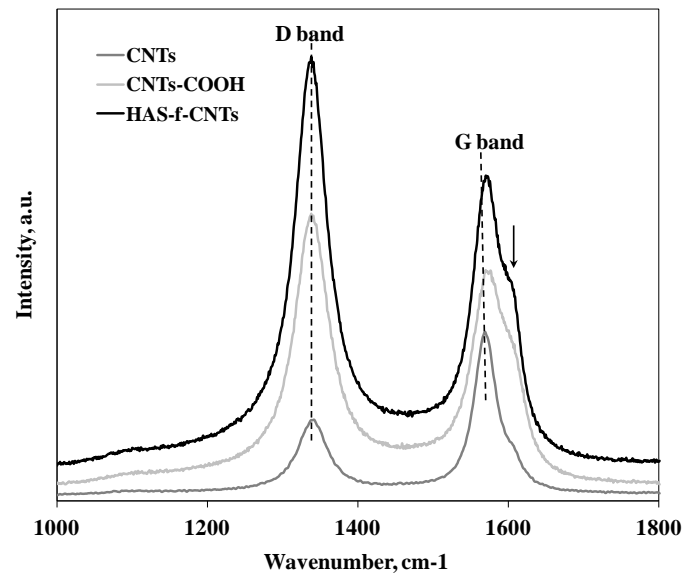


**Figure 5.** Raman spectra of bare CNTs, CNTs-COOH and HAS-*f*-CNTs

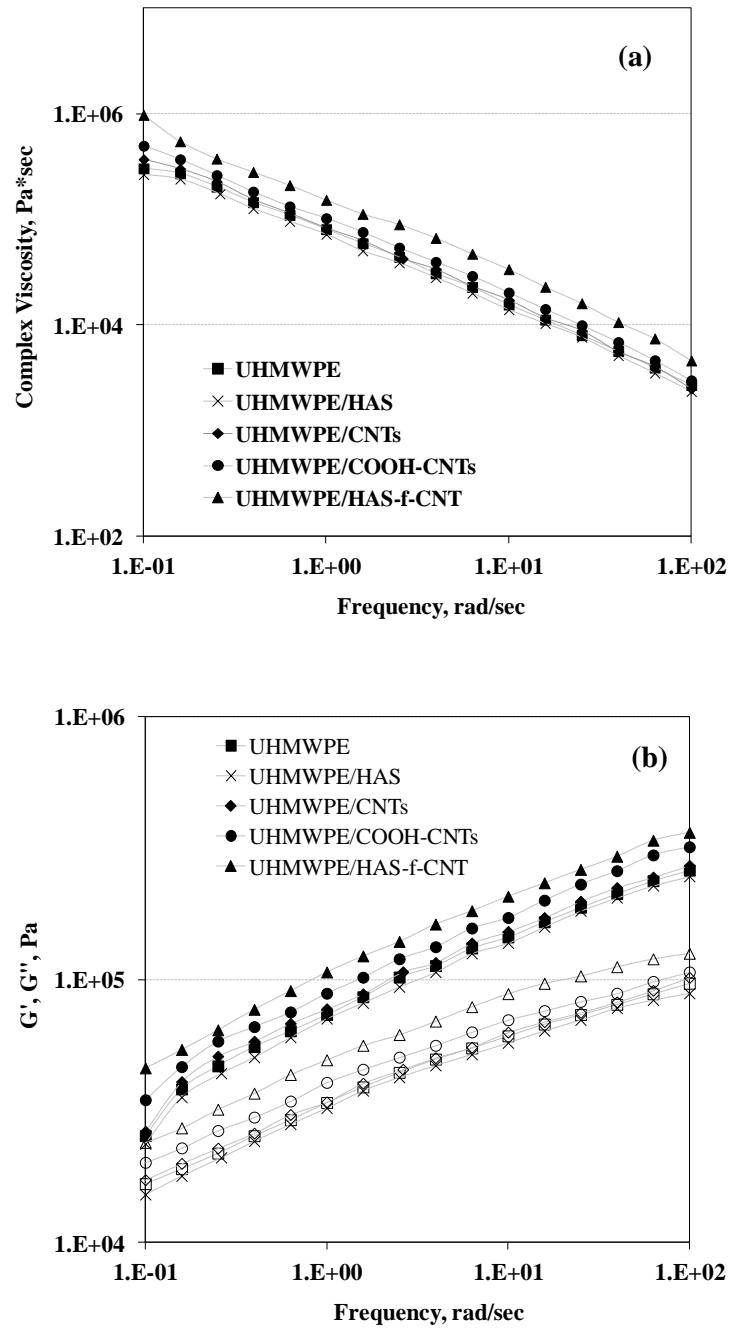


**Figure 6.** (a) Complex viscosity curves ( $\eta^*$ ) and (b) elastic ( $G'$ ) and loss ( $G''$ ) moduli of neat UHMWPE and investigated nanocomposites

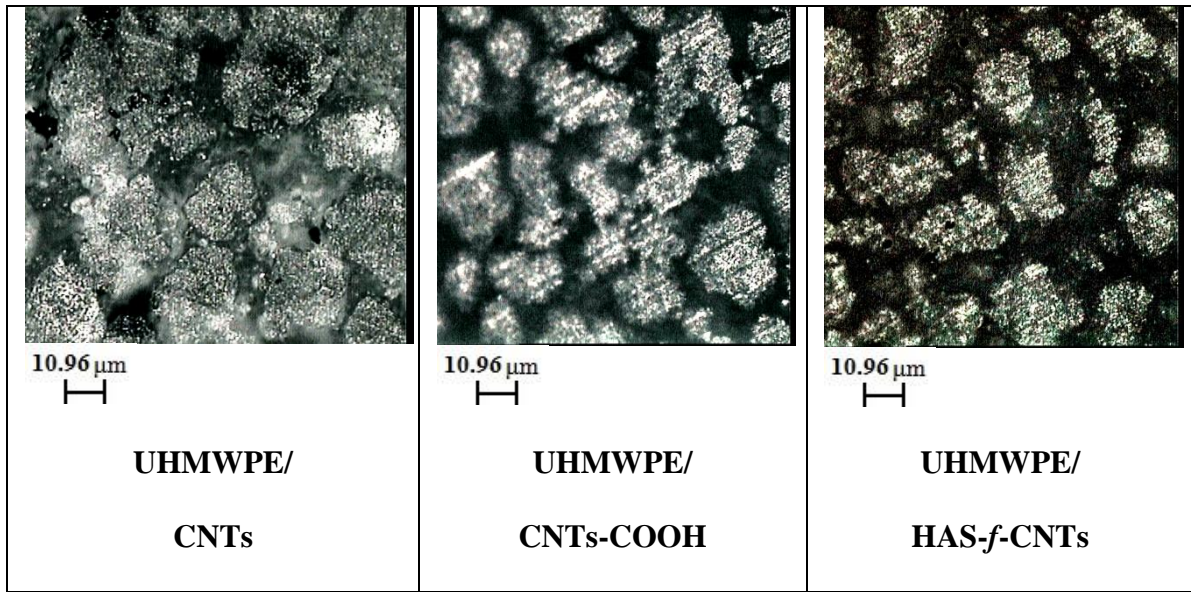


**Figure 7.** Optical micrographs of all investigated UHMWPE-based nanocomposites

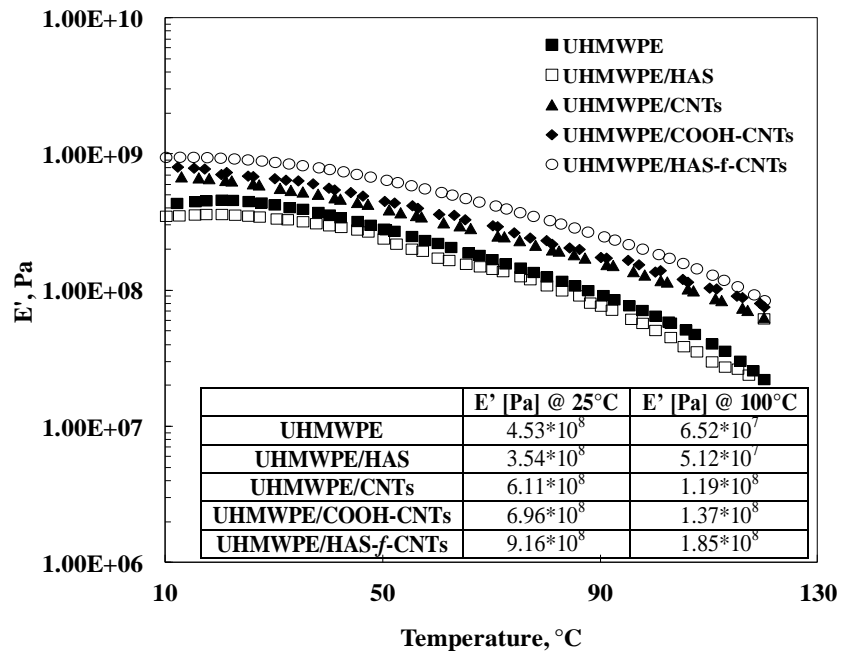


**Figure 8.** Elastic modulus  $E'$  as a function of temperature for all investigated systems

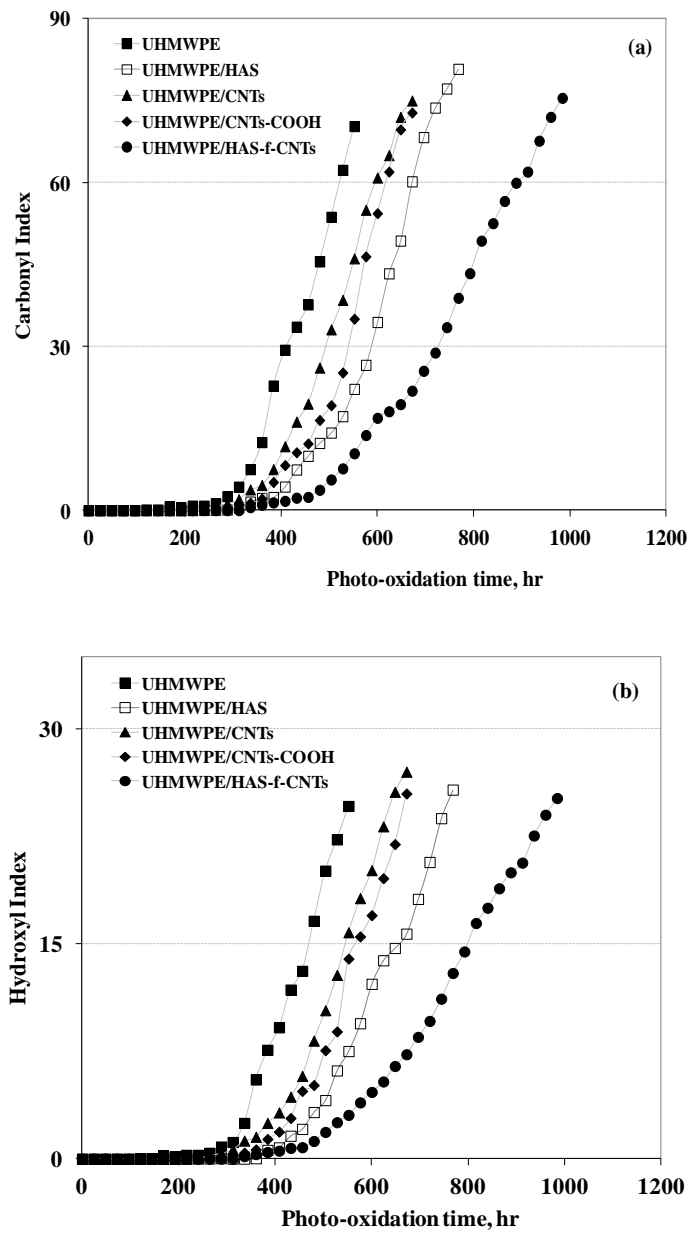


**Figure 9.** Carbonyl (a) and hydroxyl (b) indices as a function of the photo-oxidation time for all investigated systems